ADDIS ABABA UNIVERSITY
COLLEGE OF NATURAL AND COMPUTATIONAL SCIENCES
DEPARTMENT OF CHEMISTRY

DENSITY FUNCTIONAL THEORY INVESTIGATIONS OF BENZOQUINONES DERIVATIVES FIRST AND SECOND REDUCTION POTENTIAL FOR REDOX FLOW BATTERY APPLICATION

MASTER THESIS

BY

GETAHUN BAYU YIMAM

ADDIS ABABA, ETHIOPIA
August 2024

DECLARATION

I Getahun Bayou, hereby declare that the work submitted for this thesis is my original work. I have not copied from any other students' work or from any other sources except where due reference or acknowledgment is made.

Name of student: Getahun Bayou Signature: _____Date submitted: _____

Advisor: Dr. Yedilfana Setarge Signature: _____Date: _____

This Thesis is approved by Examiners and chairman of the department of chemistry for the acceptance of the thesis entitled "A Density Function Theory Investigation of Benzoquinone Derivatives First and Second Reduction Potential for Redox Flow Battery Application." This thesis has been submitted in partial fulfilment of the requirement for MSC degree in chemistry

Chairman: _____ Signature: _____ Date: _____

Examiner1: _____ Signature: _____ Date: _____

Examiner 2: _____ Signature: _____ Date: _____

ABSTRACT

Quinones are excellent candidates for organic-based redox-flow batteries due to their high redox potential. In this study, the first and second redox potentials of benzoquinone (BQ) and its derivatives were calculated using the state-of-the-art density functional theory (DFT) tool implemented in Gaussian 09 software at the theory level of B3LYP with 6-311G/d basis set and CPCM solvation model. The BQ derivatives were derived by adding EWD substituents (-CHO, -$COCH_3$, -$COOCH_3$, -CF_3, –CN, -NO_2Inaddition to the effect of functional groups, solvation free energy, and HOMO-LUMO energies and the reduction potentials was studied. The DFT results revealed that the EWD substituted BQ were found to have the highest first and second redox potentials than EDG substituted BQ. Moreover, the electrochemical behaviour of BQ and its derivatives in n-hexane (C_6H_{14}),dimethylsulphoxide (DMSO), and water solvents were studied. Due to the solvent's hydrogen bonding, polarity, and dielectric constant, the average reduction potential measurements have the following trends: n-hexane less than DMSO and water.

Keywords: Benzoquinone derivatives, Density functional theory, redox potentials, redox-flow batteries

ACKNOWLEDGMENTS

First, I would like to express my sincere gratitude to my advisor,Dr. Yedilfana Setarge for giving me constructive advice and guidance from the beginning up to the completion of this research work. I thank him because, without his encouragement, suggestions, insights, guidance, and professional expertise, the completion of this work would not have been possible. Dr. Yedilfana Setarge has an incredible ability to motivate by constantly coming up with new ideas, following up, and arranging workshops to share ideas among different scholars.

In addition, I would also like to thank material science students, computational department students, M/r Desalegn, Mr. Getachew Abera, Mr. Halid Abdu, Mr. Tolosa Tesfaye, and computational lab students for their contribution to my study.

My thanks also extend to the Ethiopian ministry of education for giving me the chance to join Addis Ababa University and for the sponsorship.

Finally, I would also like to thank my parents and friends for their great support, encouragement and emotional support.

TABLE OF CONTENTS

ABSTRACT ii
ACKNOWLEDGMENTS iii
LIST OF FIGURES vi
Figure 1 Schematic illustration of a redox flow battery [16] ..... 2 **Error! Bookmark not defined.**
LIST OF SCHEMES viii
LIST OF ABBREVIATIONS ix
CHAPTER ONE 1
1.1. INTRODUCTION 1
1.2 Background of the study 1
1.3. Statement of the problem 5
1.4.2. Specific objectives 5
CHAPTER TWO 6
2. RELATED REVIEW LITRATURE 6
2.2. Advantages and Disadvantages of Redox Flow Battery 9
2.3. Quinone-based redox flow battery 9
CHAPTER THREE 11
3. COMPUTATIONAL METHODE 11
3.1 Quantum Chemistry 11
3.1.1. Schrodinger equation 12
3.1.2. Born-Oppenheimer approximation 12
3.1.3. Density functional theory 13
3.1.4. The Hohenberg-Kohn theorem 14
3.1.5. Kohn-Sham theorem 15
3.1.6 Exchange-correlation 16
3.1.7. Local density approximation 17
3.1.8. Generalized Gradient Approximation 17
3.1.9Meta - Generalized Gradient Approximation 18
3.1.10 Hybrid-generalized gradient approximation (H-GGA) 18
3.2. Computational Details 19
CHAPTER FOUR 23
4. RESULTS AND DISCUSSION 23
4.1. Geometry optimization 23
4.2. Solvent effect 24
4.3. Theoretical first and second Reduction Potential Analysis 27
4.4. Effects of a functional group on the reduction potential of BQ 30
4.5. HOMO-LUMO energies 31

CHAPTER FIVE 37
5. CONCLUSION AND RECOMMENDATIONS 37
5.1. Conclusion 37
5.2. RECOMANDATION 38
REFERENCES 40

LIST OF TABLES

Table 1. The free energies of solvation(ΔGsolv) of BQ derivatives using water, dimethylsulphoxide and n-hexane 25
Table 2. Computed first (Ered1V and second (Ered2 V) the reduction potential of various BQ derivatives at the B3LYP/6-311G (d) level of theory. 28
Table 3**.** The HOMO-LUMO energy gap is computed at B3LYP/6-311G (d) level. 32

LIST OF FIGURES

Figure 1. Schematic illustration of a redox flow battery [16].....2
Figure 2. Two electron reductions of BQ in an aqueous buffer.....4
Figure 3. A schematic diagram of RFB [42].....9
Figure 4. Schematic diagram of "Jacob's ladder" of exchange-correlation functional proposed by J. P. Pardew [60]. 19
Figure 5. optimized structures of BQ and its derivative 24
Figure 6. The free energies of solvation(ΔGsolv) of BQ derivatives using water, dimethylsulphoxide and n-hexane 26
Figure 7. The first and second reduction potential of BQ and its substituent in water at B3LYP/DFT Using at 6-311/G (d) level of theory.....30
Figure 8. Shapes of the HOMO and LUMO orbitals of compounds 1-7 at the DFT/B3LYP/6-311/G/d level.....34
Figure 9. the computed HOMO-LUMO energies of BQ derivatives at the B3LYP/DFT level of theory using a 6-311G/d basis set. 36

LIST OF SCHEMES

Scheme 1.The thermodynamic quantity used to calculate solvation-free energy……19
Scheme 2. Structural features of BQ derivatives. 22

LIST OF ABBREVIATIONS

BQ	Benzoquinone
B3LYP	Becke, 3-parameter, Lee-Yang-Parr
CPCM	Conductor like Polarized continuum model
DMSO	Dimethylsulphoxide
DFT	Density functional theory
EA	Electron affinity
EDG	Electron donating group
E_g	Band gap
EWG	Electron withdrawing group
FMO	Frontier molecular orbital
GGA	Generalized gradient approximation
HK	Hohenberg-Kohn
H-GGA	Hybrid-generalized gradient approximation
HOMO's	Highest occupied molecular orbital
KS	Kohn-Sham
LDA	Local density approximation
LUMO's	Lowest-unoccupied molecular orbital
SCRF	Self-consistent reaction field

CHAPTER ONE

1.1. INTRODUCTION

1.2 Background of the study

Energy consumption is increasing on a daily basis, in response to a growing world population and a booming industrial development. Energy production still relies mainly on the fossil fuels that urgently requires a substitute, given in their infinite source and negative environmental impact. During the last 20 years, renewable energies have been a key element for the subsequent transition of ignition-based power plants to zero-carbon emission power sources. With the growth of renewable energy sources such as wind, hydroelectric power, solar energy and geothermal energy for large-scale energy storage devices are becoming more important to replace fossil fuels and give a reliable solution to the challenges. Renewable energy sources are predicted to become the primary energy source by 2050, with an annual growth rate of 3.6% [1], with solar and wind responsible for 70% of the total renewable production [1].Due to the intermittency of renewable energy fast and reliable energy storage devices are required for the development of the energy power supply with longer service life without putting pressure on the Earth's resources [2.3].Renewable energy sources, such as solar and wind, are promising alternatives to mitigate the energy and environmental problems associated with fossil fuels. However, one of the key challenges of utilizing sustainable energy sources is to address their distinct intermittency [4-8]. A smart grid is an attractive solution to address this problem. Under this circumstance, solving the issue of how to store and release electricity becomes a matter of urgency. Redox flow batteries (RFB) have attracted widespread attention due to their cost-effectiveness and reliability [5, 9– 12]. Highly efficient large-scale electrochemical energy storage is crucial for maintaining the stability and dependability of power networks. Redox flow batteries (RFBs) provide a better option among other electrochemical energy storage technologies in medium- to large-scale stationary applications in terms of dependability, safety, and affordability. In terms of cost, system flexibility, quick response, and safety concerns for large-scale applications, redox flow batteries show great advantages over other types of batteries such as lead-acid and lithium-ion batteries and are expected to have increasing commercial space through technological development in the future. The redox flow battery is thought to be

appropriate for large-scale applications because of its modular architecture, good scalability, and flexible functioning.

Steadily increasing utilization of renewable energy resources, such as solar and wind power, requires affordable and sustainable energy storage technologies at grid scales up to MW/MWh [13, 14] Redox flow batteries (RFBs) represent one of the most promising battery technologies to overcome the intermittence of renewable energy and supply reliable renewable electricity to grids.[13,14] Simultaneously, the implementation of renewable electricity will significantly address the dependence on diminishing fossil fuels and their adverse environmental impact. The distinctive cell architecture of RFBs empowers several attractive technical strengths for large-scale energy storage in comparison to traditional static cells, including decoupled energy and power, high current and high power performance, and safety advantages [13 -15].

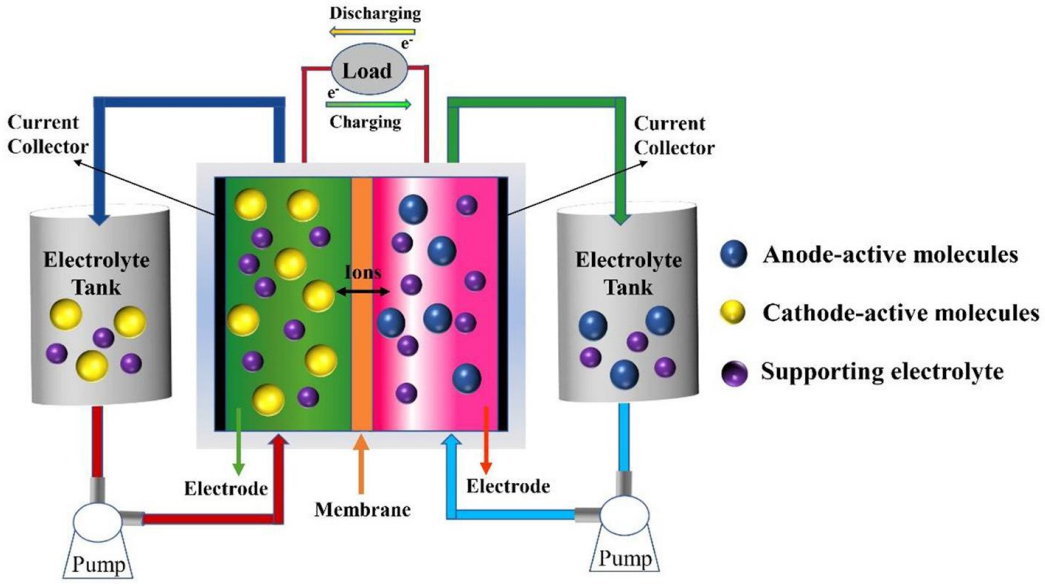

Figure 1. Schematic illustration of a redox flow battery [16]

In a redox flow battery, the redox-active species is the most significant component. The energy and power of the system are determined by the redox potential and solubility of electro-active species. The energy density in the two half-cells is determined by the number of electrons transferred, the concentration of electro-active molecules, tank size, and the active species' equilibrium potential [17]. The power rating is determined by the cell electrode area and the number of cells in the stack. The chemical stability, electrochemical reversibility, and reduction potential of redox materials all contribute to the overall performance of redox flow batteries.

The performance of RFBs is mainly determined by their energy density and cycling stability. The theoretical energy density, which indicates the amount of charge stored, is calculated from the following Equation 1.

$$\text{Energy density (Wh/L)} = nCFV/\mu v \qquad 1$$

Where, n = is the number of electrons transferred in the redox reaction, C= is the lower concentration of the redox-active materials from either the negolyte or catholyte in mol/L, F= is the Faraday constant, V =is the cell voltage, and μv= is the reduced volume factor and is equal to the 1 + (max concentration of less soluble electrolyte)/ (max concentration of more soluble electrolyte).

This equation explicitly shows three core parameters of (1) cell voltage, (2) solubility, and (3) multiple electron transfer, which governs the functioning of RFBs [18]. Some parameters can be used to assess an RFB's battery performance. First, battery voltage, which represents the maximum driving force that a battery can give, is one of the most fundamental and significant factors for EES devices. The redox potentials of the anolyte and catholyte dictate the theoretical battery voltage, but the actual open circuit over potential is further influenced by a flow battery's internal resistance and the electrochemical kinetics of redox-active materials. The following equation [19] defines an electrolyte's theoretical capacity (abbreviated Ct) as the amount of charge (Ah) stored in a specific amount of electrolyte:

$$\text{Capacity (Ct)} = \frac{nF}{3.6Mw} \qquad 1.1$$

Where n = is the number of electrons involved in a redox reaction, F= Faradays constant and Mw= the molecular mass weight of a substance

Because of their abundance on the planet and ease of processing, redox-active organic compounds are becoming increasingly popular in sustainable development and energy storage systems. Organic redox flow batteries are environmentally friendly and structurally diverse. Quinones perform two-electron redox reactions in an aqueous solution, allowing Quinone-based flow batteries to reach higher energy densities than traditional flow batteries.

The electrochemical redox potentials of benzoquinone derivatives were carried out either in aqueous or non-aqueous solutions using the CPCM solvation model. The electrochemical reduction potential of benzoquinone and its substituent takes place through two successive step-by-step one-electron reductions and a formation of two separated cathodic waves. The

first step of reduction potential corresponds to the formation of benzoquinone anion,BQ^{-} while the second reduction step is in the formation of benzoquinone dianion,BQ^{-2}.

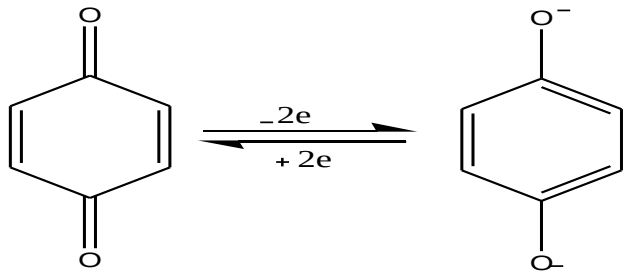

Figure 2. Two electron reductions of BQ in an aqueous buffer

In a reversible redox process, Quinone derivatives are the most promising organic electrode materials. The electrochemical potential of the studied substance should be determined using CPCM, solvation models in both aqueous and non-aqueous solutions. Quinones undergo a first one-electron reduction step in neutral aprotic environments to form the semi-quinone radical anion, which is followed by a second one-electron reduction step to produce the hydroquinone dianion. For aqueous electrolytes, side reactions such as hydrogen evolution (common in acids), and oxygen evolution (common in alkaline solutions) by electrolysis of water take place during charging at very positive and negative electrode potentials respectively., and other degradation of electroactive molecules catalyzed by acid and base; being non-corrosive, non-flammable, environmentally benign and neutral aqueous supporting electrolytes eliminate side reactions, NaCl [20 - 22].

In electrochemistry, computational chemistry is a powerful tool, and as a result, it is competitive in experiments for obtaining certain chemical properties. When experimental observations are problematic, the inclination to calculate the redox potential properly using the theoretical method is favorable. Gaussian09 software was used to optimize all geometries of the studied compounds both in gas and solvent phases. The redox potentials of BQ's first and second reduction potentials were computed in both aqueous and non-aqueous solutions using the conductor-like polarizable continuum model (C-PCM).

The solvation energy, functional group effect, and HOMO-LUMO energies on BQ molecules and their derivatives should be computed. As well as the contributions of the EA and solvation energy to the redox potential are systematically studied.

1.3. Statement of the problem

Fossil fuels are treating the globe causing different environmental problem. The application of renewable electricity will significantly address the dependence on diminishing fossil fuels and their hostile environmental impact. To reduce the energy and environmental problems associated with fossil fuel a large scale energy storage devices are required to replace fossil fuel. Redox flow batteries provide a better option among other energy storage devices.

The RFBs empowers several attractive technical strengths for large-scale energy storage in comparison to traditional stationary batteries, including high current and high power performance, decoupled energy and power, and safety advantages.

This thesis focus on improving the energy storage capacity of a redox flow batteries by introducing electron-withdrawing groups in the ortho position of benzoquinone molecule for redox flow battery application.

1.4.1. General objective

The main purpose of this study is to evaluate the theoretical first and second reduction potentials of benzoquinone and benzoquinone derivatives by introducing EWGs in the presence of various solvents and salts by Gausian09 software, the density functional theory method at B3LYP level of theory using a 6-311G/d basis set, and conductor-like polarizable continuum model (C-PCM) approach was used to include the role of the solvents.

1.4.2. Specific objectives

- To identify a key descriptor used to calculate the reduction potentials of benzoquinone and its derivatives.
- To examine the first and second reduction potentials of benzoquinone by introducing different electron-withdrawing groups in the presence different solvents.
- To study the effect of various electron-withdrawing group to BQ's chemical reactivity.
- To study the effect of the various solvents on the solubility and stability of benzoquinone and its derivatives.

.

CHAPTER TWO

2. RELATED REVIEW LITRATURE.

In line with the expected substituent effects from qualitative considerations of chemical bonds and electron densities, Er et al. [23] determined the order of the reduction potentials for single and fully substituted BQ, NQ and AQ derivatives for aqueous redox flow batteries according to -OH<- Me<- OMe<-H<-F<- SO3H<-CN, -NO2. This qualitative trend is also in agreement with the available experimental data for Qs with - SO3 and -OH substituents.[24] Furthermore, it has been shown for diaza-anthraquinones and dihydroxy-phthalazines that -OMe, -Me and -OH result in redox potential lowering [25,26]. General chemistry concepts indicate that methyl substituents have a positive inductive effect, which should lower the redox potential. The BQ derivatives show the highest redox potentials among the Q derivatives due to the smallest ring size. An increase/ decrease of this redox potential due to substituent effects.

Along our expectation of electron withdrawing and donating effects, there is a redox potential increase for BQ derivatives with - NO2, - CN, -SO3 substituents compared to BQ, whereas the redox potentials decrease for BQ derivatives with - OH, - Me, -OMe substituents.[24].

Substitution of quinone hydrogen with EDGs, such as –OH, $-NH_2$, $-N(CH_3)_2$ decreases the electron affinity of the compounds and results in low reduction potential values. Functionalization with EWGs such as – SO_3H, $-COOCH_3$, -CHO, -COOH, $-CF_3$, -CN and – NO_2, shows an opposite effects and results in high redox potential values [27].

The ordering of the functional groups correlates with the nature of EDGs and EWGs and trends from molecular induction theory and Hammet parameters [28]. EDGs decreases the reduction potential significantly when compared to unsubstituted parent benzoquinone. Conversely EWGs, are useful in increasing the redox potential.

The critical factor in tuning the electrochemical properties of quinone is the position of the substituted groups on the benzoquinone backbone [29-31]. The substitution of –OH group adjacent to the ketone decreases the redox potential more effectively than their substitution with remote benzoid ring hydrogen. Similarly, the effect of –CHO, -CN, COOH, $COOCH_3$, CF_3, NO_2 groups increases the redox potential when substituted for the quinone hydrogen adjacent to the ketone unit.

As it was done in previous paper the reduction potential of EDGs substituted benzoquinone, using SMD solvation model the investigation report shows EDGs has lower redox potential as compared with recently I did in EWGs substituted benzoquinones.

A redox flow battery, like a typical battery or fuel cell, is an electrochemical energy storage device that converts the chemical energy of electro-active species directly into electrical energy. The electro-active species, on the other hand, is stored outside. In RFB; catholyte and anolyte are the redox active compounds dissolved in electrolyte solutions and stored in two different tanks with volumes selected as needed for the application. The core of the battery where redox reactions occur is called the stack, which can also be scaled as large as necessary for custom power requirements. Due to the unique system, many tanks connect to one stack and the solution can travel by pumps. This arrangement is effective for changing the input chemicals, long-term use/maintenance, and ideal for large-scale applications The fundamental properties of redox flow batteries are the ability to decouple energy and power in the electrolyte tank and a stack, respectively (tank size is related to energy and number of stack is to power.

There are two main classes of RFB depending on the solvent in which the active compounds are dissolved: aqueous and non-aqueous organic redox flow batteries [32]. AORFBs have several outstanding advantages for large-scale energy storage, five of which are outlined here [33]. (1) Using organic redox-active molecules consisting of earth-abundant elements is a sustainable practice. (2) Redox-active molecules are also synthetically tunable to gain high oxidation or low reduction redox potentials and can have high solubility, thus offering high energy density RFBs while providing optimal membrane compatibility. (3) Utilization of non-flammable aqueous electrolytes offers safety benefits. (4) Aqueous electrolytes consisting of water and simple inorganic supporting electrolytes, such as NaCl and KOH, are inexpensive. (5) High-conductivity aqueous electrolytes (>100 mS/cm) and well-developed selective ion conductive membranes for aqueous electrolytes allow high-current and high-power operation while achieving high energy efficiency. On the other hand, aqueous solutions offer a high dielectric constant for high solubility of active compounds and background electrolytes (for solution conductivity) and very low cost. The most promising energy storage candidates to clear the aforementioned challenges of performance, cost, and environmental sustainability are aqueous organic redox flow batteries [34-37]. However, aqueous electrolytes have a limited potential window (about 1.8 V in practice) due to the electrolysis of water [38]. High standard reduction potential, high solubility, a large number of electron transfers, fast reaction kinetics, and good reversibility are some of the most

enticing characteristics of aqueous organic redox flow batteries [19]. The fundamental properties of redox flow batteries are the ability to decouple energy and power in the electrolyte tank and a stack, respectively (tank size is related to energy and the number of stacks is to power. Their scalability, flexibility in modular design and operation, long life cycle, and low costs differ from other types of batteries [33].

2.1. Working principles of redox flow battery

A redox flow battery converts energy from electrical to chemical and vice versa. This inter-conversion occurs in the electrochemical cell, according to [39-41]. Liquid electrolytes are pumped from storage tanks to flow across an electrode in a cell stack, where the conversion takes place. The redox reaction of electro-active materials dissolved in supporting electrolyte, which circulates between the tanks and corresponding compartments of the electrochemical cell and is powered by external pumps at the electrodes, which allows chemical energy to be converted into electric energy. To complete the current circulation, certain ions pass the ion-exchange membrane. The potential differences between electro-active species during cathodic and anodic half-cell reactions, as well as the number of electrons transferred between the two electrolytes, which is used to determine the cell voltage. Figure (2) below depicts a general redox reaction mechanism for the anode and cathode during charging/discharging modes [42]. During discharge, an electron is liberated from a high chemical potential state on the battery's negative or anode side via an oxidation reaction. The electron performs beneficial work by moving through an external circuit. Finally, the electron is accepted on the positive or cathode side of the battery via a reduction reaction at a lower chemical potential state. During charging, the current and chemical processes are reversed.

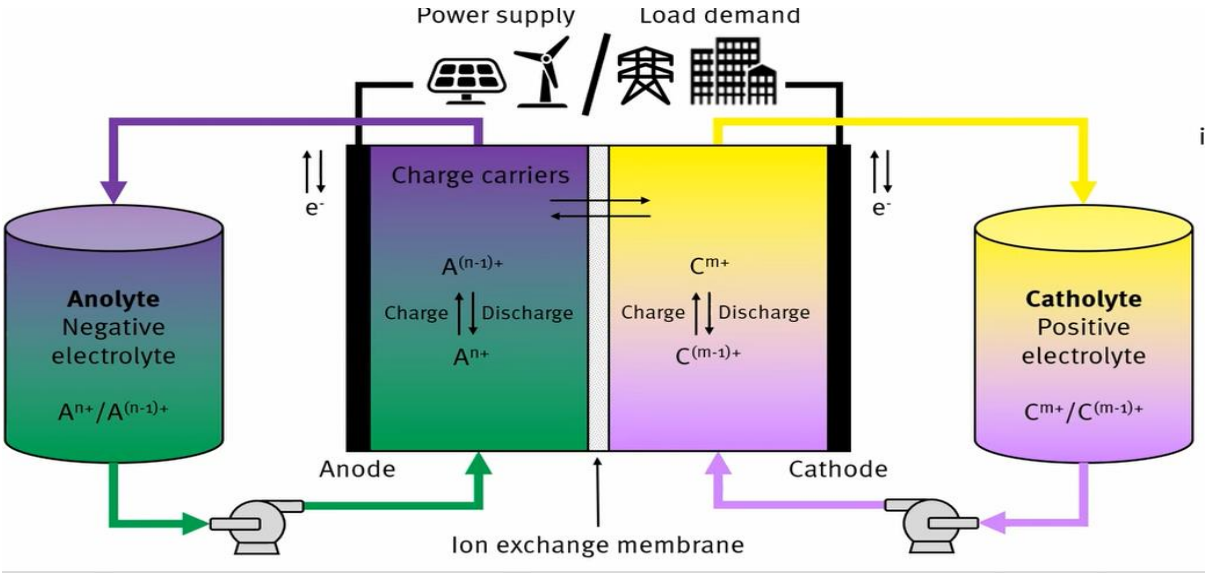

Figure 3. A schematic diagram of RFB [42]

2.2. Advantages and Disadvantages of Redox Flow Battery

A conventional battery such as the lithium-ion battery is restricted in its size and capacity, which is not favorable for large-scale energy storage. Separated tank and stack is a big advantage of RFB, maximize their performance by adding more tanks or increasing the stack size. In the long term, using active compounds could easily be substituted after many years of service by exchange the electrolyte tank fluid. Another advantage of aqueous RFB is safety. Active compounds are dissolved in water and transported into the stack for electron transfer, in comparison to Li-ion battery design; the risks of overcharge or over discharge reaction are minimized, which may lead to overheating and explosion in organic solvent-based batteries like Li-ion.

The drawback of the redox flow battery is the system. RFB system is complex as there are pumps, sensors, flow tubes, power management, stacks, and tanks. A single broken part might hurt the whole system, so maintenance fees should be factored in for RFB.

2.3. Quinone-based redox flow battery

Quinone-based organic compounds have expected great consideration ranging from benzoquinone to anthraquinone. Because of their high reversibility, low cost, ease of

availability, environmental friendliness, and quick reaction kinetics, these materials offer a important advantage over metal-based redox flow batteries. The development of organic redox-active materials for redox flow batteries holds great promise for stationary electrochemical energy storage.

Quinone is an organic electro-active molecule that can function as a positive or negative electrolyte. Quinone undergoes a reversible two-electron reduction in aqueous environments, with a reduction potential that varies with pH [43]. Quinones undergo a one-electron reduction step in neutral aprotic environments to form the semi-quinone radical anion, which is followed by a second one-electron reduction step to produce the hydroquinone dianion [44]. Electron transfer reactions are very important to predict accurate redox potentials of Quinones [45]. Computational chemistry is a powerful tool in electrochemistry to predict the redox potentials of Quinones [46]. The most common approach for computing the redox potentials is the use of thermodynamic cycle which involves gas-phase free energies and solvent-phase free energies of solvation [47].

CHAPTER THREE

3. COMPUTATIONAL METHODE

Computational science has been designed for some decades to study molecular structure and solve chemical problems. The advantage of computer simulations is in time and cost savings in a wet laboratory. Due to the expense and difficulty of wet lab experiments, performing computational experiments and predictions is excellent for studying molecular transformations, predicting/interpreting spectroscopic data, frequency calculation, potential energy surface, geometry optimization, transition structure and redox potential energy. In computational science, there are mostly two major classes of calculations: molecular dynamics and quantum mechanical approaches. In molecular dynamics, atom and molecules are simulated on a computer to obtain their physical movements.

3.1 Quantum Chemistry

Quantum Chemistry (QC) is a branch of chemistry focuses on determining the electron structure within atoms and molecules. Specifically, QC is theoretical chemistry, and it calculates a molecule's properties including geometry, electronic energy, electric dipole moment, charge distribution, vibrational frequency, etc…,[48]. Then, it can be used to predict the mechanism of reactions and analyse electronic reorganization during the reactions. In the history of computational chemistry, different programs, algorithms and models for simulating electronic structure have been created depending on the purpose of research and systems under study. Hence, it is important to understand and select the appropriate methods to model and analyse molecule while saving time and computational resources (cost). In QC Schrödinger equation is used to describe characteristic of electron:

$$\hat{H}\boldsymbol{\psi} = E\boldsymbol{\psi} \qquad (3.1)$$

Where, $\boldsymbol{\psi}$ is the wavefunction, $\hat{H}$ is the Hamiltonian operator and $\boldsymbol{E}$ is the energy of the given system. Application of $\hat{H}$ to the wavefunction determines the energy of system, *E*, known as the eigenvalue to the Hamiltonian. The major goal in computational chemistry calculations is solving the Schrodinger equation to determine the minimum energy of a chemical system.

Three different methods to approach solution of this equation: *Ab initio*, semi-empirical and Density Functional Theory (DFT).

3.1.1. Schrodinger equation

The basic principle on which DFT lies is the Schrodinger equation which defines how the quantum state of a physical system changes in time. The electronic properties of many atoms were investigated. To establish the properties of a large number of electrons, we must solve as many body systems as possible and construct Hamiltonian, H, before solving the Schrodinger equation [49].

$$\widehat{H}\Psi = E\Psi \quad (3.2)$$

Where H is the Hamiltonian operator (r_1, r_2, ...) for many-body wave functions based on electron spatial coordinates, and E denotes the system's electrical energy. Only up to one electron system, we solve for Schrodinger equation exactly. For a system of p electrons and P neutrons atoms, many-body Hamiltonian operators are as follows:

$$E\Psi(r,R) = T_N + T_e + V_{ee}(r) + V_{NN}(R) + V_{eN}(r,R)]\Psi(r,R) \quad (3.3)$$

$$\mathbf{H} = \boldsymbol{T_e} + \boldsymbol{T_n} + \boldsymbol{V_{n-n}} + \boldsymbol{V_{n-e}} + \boldsymbol{V_{e-e}} \ (\mathbf{3.4})$$

$$H = -\frac{\hbar^2}{2}\sum_{\alpha}\frac{\nabla_{\alpha}{}^2}{M_{\alpha}} - \frac{\hbar^2}{2M_e}\sum_i \nabla_i^2 + \sum_{\alpha}\sum_{\beta>\alpha}\frac{Z_\beta Z_\alpha e^2}{4\pi\varepsilon_0 r_{i\alpha\beta}} - \sum_\alpha \sum_i \frac{Z_\alpha e^2}{4\pi\varepsilon_0 r_{i\alpha}} + \sum_{i>j}\frac{e^2}{4\pi\varepsilon_0 r_{i\alpha}} \quad (3.5)$$

Both T_e and T_n are the kinetic energy of an electron and nuclei, respectively. The potential energy contribution or columbic interaction is represented by the next last three terms: nuclei-nuclei (V_{n-n}), nuclei-electron, (V_{e-n}), and electron-electron (V_{e-e}), respectively. Except for the one-electron system, solving the Schrodinger equation directly is challenging due to interaction factors.

3.1.2. Born-Oppenheimer approximation

Because of big difference in mass between electrons and nuclei, the electron's motion is much faster than nuclei and assumed that the nuclei are stationary. Then, the nuclear kinetic

energy is assumed as zero. And the nuclei- nuclei repulsion does not change (is constant). Hence, the Hamiltonian is reduced into a simpler form. As a result, it's critical to distinguish electrostatic interactions between nuclei and electrons. The Born-Oppenheimer approximation is a mathematical assumption that separates the velocity of the electron from that of the nucleus and considers them separately [50]. It is the foundation for practically all electronic computations. The Schrodinger equation for many-electron wave functions can be simplified using the Born-Oppenheimer approximation, as shown in the equation:

$$H\psi = (T_e + V_{e\text{-}n} + V_{e\text{-}e})\psi = E\psi_e \quad 3.6$$

The Born-Oppenheimer approximation is a cornerstone of computational chemistry because it introduces molecular geometry meaningful, makes possible the concept of the potential energy surface, and eventually simplifies Schrodinger's equation to molecules by allowing us to focus just on electron-electron interactions.

3.1.3. Density functional theory

The quantum mechanical method of density functional theory (DFT) is used to calculate the electronic structure of atoms, molecules, and solids. The electron density n(r) of a species is determined using density functional theory [51]. It is one of the best effective methods for determining a material's electronic structure, and it is mostly based on the electron density, which determines a system's energy in the ground state. The electron density is the most essential parameter in DFT calculations since n(r) describes a function in real space and makes the result easier to understand. For density functional theory, a variation approach can be established. The first breakthroughs in the development of modern DFT, via the Hohenberg-Kohn theorems and the work of Kohn and Sham, were developed. DFT calculations are popular recently due to its computational efficiency and accuracy, with results approaching the accuracy of *Ab initio* and semi-empirical but with significantly faster processing times. That is the reason why a lot of research is applying DFT in recent years [52].

DFT is a method that enables approximates, precise, and economical solutions to a Schrödinger equation. As a result of the DFT calculation, ground state electronic energies and wave functions can be calculated. The ground state density and total energy could be determined exactly if we know the values of each term in the Kohn-Sham energy functional. The exchange-correlation (XC) functional is unluckily one unknown term (E_{XC}). Exchange-correlation contains both the component of kinetic energy that differentiates the real system

from the hypothetical non-interacting system as well as the non-classical aspects of the electron-electron interaction. It is necessary to approximate E_{XC} because it is not known exactly

3.1.4. The Hohenberg-Kohn theorem

In DFT calculation, Hohenberg-Kohn theory (1964) is used to explain electron density [53]. The first Hohenberg–Kohn theorem states that 'the ground state of any interacting many particle systems with a given fixed inter-particle interaction is a unique functional of the electron density n(r). The electron density of any system determines all ground-state properties of a system. To solve the Schrodinger equation, Hohenberg-Kohn had to propose two essential theorems, each of which provided a theoretical foundation for electron density rather than many bodies' wave functions. Only three coordinates determine the density of electrons. As a result, the number of variables in a 3N coordinate system can be reduced to an N-electron system. The first theorem of HK, the total ground state of many electron systems is a function of the electron density. So, if we know the electron density functional, we know the total energy of our system. HK states that "the ground state electronic energy from Schrodinger equation and other properties like atoms or molecules are determined by electron density." The ground state energy, E, can be written as a function of electron density n(r).

$$E_0 = F[(n(r)_0)] = E[(n(r)_0] \quad (3.7)$$

In Hohenberg and Kohn's formalism, the ground state electronic energy can be expressed as:

$$E[(n(r))] = T[n(r)] + V[n(r)] + U[(n(r))] \quad (3.8)$$

Where, T[n(r)], represents the kinetic energy component, V[n(r) potential energy due to static nuclei, and U[n(r) electron-electron interaction. The second theorem of HK, states that the true ground state density of an electron corresponds to electron density that minimizes the overall energy of the functional. So, this theory declares that any trial electron density will be more than or equal to the ground state energy (real electron density). The ground state energy is calculated by minimizing n(r) over three-dimensional functions about the energy functional. The variation principle governs the second theorem of HK of electron density.

$$E_0 = \min_{n(r)} E[n(r)] \quad (3.9)$$

This equation demonstrates that n(r) minimizes the energy functional E(n(r)

3.1.5. Kohn-Sham theorem

Many-body problems can be reduced to a single electron problem using Kohn and Sham's [54] equations. Kohn and Sham presumed that the reference system's ground-state electron probability density is equal to the exact ground-state electron density. A set of imaginary non-interacting electrons serves as a starting point for solving the KS equations. The local effective external potential, generally abbreviated as (r), in which the fictitious electron moves, is defined by the Kohn-Sham equations. To obtain orbitals that give rise to the ground state energy, we must minimize the total energy concerning orbit using the Hohenberg-Kohn theorem. The energy functional of the KS equation can be written as:

$$E[n(r)] = V[n] + U[n] + G[n] \tag{3.10}$$

Where G[n] is universal density functional which holds exchange-correlation and it can be written as follows:

$$G[n(r)] = T_S[n] + E_{XC}[n] \tag{3.11}$$

$$\text{Then, } E[n(r)] = T_S[n] + V[n] + U[n] + E_{XC}[n] \tag{3.12}$$

Where $T_S[n]$ is the kinetic energy of many-body systems having non-interacting electrons.

$$T_S[n] = -\frac{\hbar^2}{2m}\sum \int \Psi i^* \nabla^2 \Psi i d^3 r \tag{3.13}$$

V[n] is columbic -interaction between electron and nuclei (having core positive charge)

$$V[n] = \int V(r)n(r)dr \tag{3.14}$$

U[n] is columbic potential as a result of electron-electron repulsion;

$$U[n] = \frac{e^2}{2}\int \frac{n(r)n(r)}{|r-r|} dr dr' \tag{3.15}$$

By introducing the wave function, Kohn and Sham were able to convert a set of many bodies' problems into a single Schrödinger equation. As a result, the equation above can be rewritten as follows:

$$\epsilon_i\Psi(r) = -[\frac{\hbar^2}{2m}\nabla^2 + V(r) + V_H(r) + V_{XC}(r)]\Psi_i \qquad (3.16)$$

The eigenvalue of orbital energy is and the KS containing non-interacting electrons is provided by the wave function, Ψ(r), and V(r). Where V(r) is the potential that determines how electrons interact with atomic nuclei. In the Hartree potential problem, V_H stands for columbic repulsion between the electron and the total electron density specified by all electrons.

So, $$V_H(r) = e^2 \int \frac{n(r)}{|r - r'|} d^3r' \qquad (3.17)$$

Then, the effective potential,

$$V_{eff} = V(r) + V_H(r) + V_{XC}(r) \qquad (3.18)$$

Since the Hartree term and V_{XC} depend on $n(\mathbf{r})$, which in turn depends on the ψi, which in turn depends on V_S, the problem of solving the Kohn–Sham equation has to be done in a self-consistent way.

The effective potentials depend on the density and indirectly on the orbitals. The equation for one particle that is non-interacting in potential can be derived from the equation of interacting electrons of a system in the presence of V(r). So, the minimization of the energy functional for n(r) yields an eigenvalue problem in the Kohn-Sham equation. This KS equation has a single particle Schrodinger equation and can be written as

$$\epsilon_i\Psi(r) = [T + V_{eff}]\Psi(r) \qquad (3.19)$$

The exchange-correlation energy, $E_{xc,}$ compensates for the electronic energy that isn't included in the non-interacting kinetic energy and electrostatic components. An effective potential is required to compute the non-interacting kinetic energy, to which the imaginary particles are exposed. The related electrostatic potentials account for the electrostatic interaction terms, while accounts for the exchange-correlation potential. The following equation is used to determine the exchange-correlation potentials that can be connected to the exchange-correlation energy functional:

$$\boldsymbol{V_{xc}(r)} = \frac{\partial \boldsymbol{E_{xc}(r)}}{\partial \boldsymbol{n(r)}} \qquad (3.20)$$

3.1.6 Exchange-correlation

In the KS scheme, just one critical difficulty is that (exchange-correlation energy) cannot be computed exactly. If exchange-correlation is determined accurately, it is a precise solution for

a many-body problem. There is currently no such exact solution exists, hence approximations are employed to estimate with LDA and GGA being the most commonly used approximations

3.1.7. Local density approximation

Kohn and Sham introduced the Local Density Approximation (LDA) [55], which argues that the exchange-correlation functional at each place in space is simply reliant on the spin density of that region. The electron density can be considered as a homogeneous (uniform) electron gas to approximate. The total energy functional can be determined by approximating the electron-electron interaction. The exchange-correlation energy can be calculated using LDA as follow;

$$E_{XC}^{LDA}[n] = \int \varepsilon_{xc}^{homo}(n(r)n(r)dr \quad (3.21)$$

Where$\varepsilon_{xc}^{homo}(n(r)$ is the exchange-correlation energy per particle of a uniform electron gas of density,n. The LDA exchange part Ɛx (n(r)) is represented by the known exchange energy of one electron in a homogeneous electron gas at a particular density:

$$\varepsilon_x(n(r)) = -\frac{3}{4}(\frac{3}{\pi})^{\frac{1}{3)}}(n(r))^{\frac{1}{3}} \quad (3.22)$$

Thus, the LDA exchange yields:

$$E_{XC}^{LDA} = -\frac{3}{4}(\frac{3}{\pi})^{\frac{1}{3)}}[n(r)]^{3/4}\,\mathrm{dr} \quad (3.23)$$

The LDA approach is an excellent approximation for features such as vibrational frequencies, structural geometries, and a wide variety of physical systems. This function makes it difficult to define molecular binding energies, chemical reaction energies (thermo-chemistries), and dissociation energies.

3.1.8. Generalized Gradient Approximation

The LDA assumption that all electrons are same leads to underestimation of the exchange energy and over-estimation of the correlation energy. To fix this problem, the spatial gradient of the electron density was added to equation which extends this calculation to more realistic non-homogeneous electron densities. The new form of GGA is [56].

$$E_{XC}^{GGA}[n\downarrow,n\uparrow]=\int\varepsilon(n\downarrow,n\uparrow,\nabla n\downarrow,\nabla n\uparrow)n(r)d3r \quad (3.24)$$

Where $n\downarrow$, $\uparrow$ illustrate spin-up and spin-down densities. Perdew and Wang [30] successfully produced highly accurate atomization energies and extended it to various system. Within each approximation method, various specific functional have been developed to treat chemical systems. Examples of commonly used GGA functional are BP86 [57], BLYP [57],[58], PW91[59], PBE [56].

3.1.9Meta - Generalized Gradient Approximation

According to Perdew [60], one problem of GGA functional is electron's self-interacting error. Each electron interacts with the total electron density and itself. Meta-GGA is an improvement of GGA but still maintains all GGA features. The most popular approximation of Meta-GGA is TPSS which was found by Tao, Perdew, Staroverov, and Scuseria. Recently, it has been applied to study equilibrium geometries, bond energies, spin-inversion, and excited energy of transitional metal system. In an article of Jensen [61].

3.1.10 Hybrid-generalized gradient approximation (H-GGA)

The Hartree-Fock theory describes the accuracy of finding an approximation to the exchange-correlation potential in the combination of GGA with a percentage exchange in a hybrid-generalized gradient approximation (H-GGA). The resultant energy functional of B3LYP's exchange-correlation energy is:

$$E_{XC}^{B3LYP}[n] = (1-a)E_X^{LSDA} + aE_X^{HF} + bE_X^{B88} + (1-c)E_C^{LSDA} + cE_C^{LYP} \quad (3.25)$$

Where, E_X^{HF} is the Hartree-Fock exchange energy, E_X^{LSDA} the local spin density approximation, B88 the Becke's exchange functional, *a*, *b*, and *c* are semi-empirical parameters and the corresponding values are 0.20, 0.72, and 0.81, respectively. The LYP term corresponds to the Lee Yang Parr correlational functional [62].

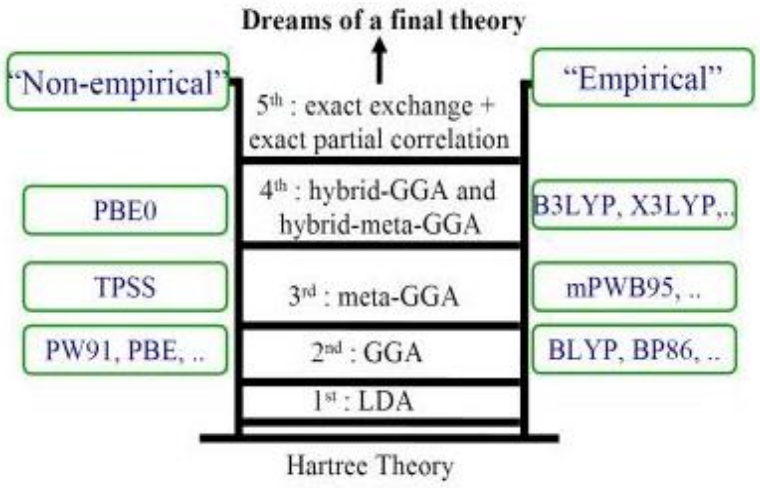

Figure 4. Schematic diagram of "Jacob's ladder" of exchange-correlation functional proposed by J. P. Pardew [60].

3.2. Computational Details

All the computations were performed using Gaussian 09 software [63]. Geometry optimizations and frequency calculations were carried out using DFT in combination with the B3LYP[62]. functional level of theory with a split-valence 6-311G/d basis set. The conductor-like polarizable continuum model (C-PCM) approach was engaged to include the role of the solvent [64]. From the optimized geometries, No imaginary vibrational frequencies were found which an indicator of true minima of the potential energy surface. Combining the optimized gas-phase free energy with the free energy of solvation yields the free energy of a solution in the reaction. . The most extensively used functional in computing DFT is B3LYP due to describing many chemical properties of matter.

The rationale for selecting the B3LYP functional was based on the fact that it is the best for studies involving main group thermochemistry, kinetics, non-covalent interactions, and electronic excitation energies. The nature of all the optimized structures is determined based on the harmonic vibrational frequency calculations determined at the same level of theory to confirm that a minimum on the potential energy surface was achieved under the imposed constraint of the indicated symmetry.

Before computing the standard redox potential, it is possible to calculate the gas phase electron affinity defined as the enthalpy change of the following reactions in the gas phase at 298K and 1atm according to the following reaction.

For the general reaction; $BQ_{(OX)} + ne^- \rightarrow BQ^-_{(red)}$

$\Delta G = \Delta G^0 + RT \ln Q = \Delta G^0 + RT\ ln\left(\frac{red^0}{ox^0}\right)$ (3.3.1)

The electrode potential, E, can be used to express the quantity of free energy produced by electrochemical cells as well as the amount of energy required to do work.

$$\Delta G_{rxn}{}^0 = -nFE^0 \quad (3.3.2)$$

Where,ΔG^0_{rxn}denotes the Gibbs free energy of solvation, n denotes the number of electrons transferred during charging/discharging**, F** denotes Faraday's constant, and**E^0** denotes the cell's electrochemical redox potential. The standard reduction potential is calculated using the reaction's standard state Gibbs free energy, and it can also be measured to the reference electrode's potential. A Conductor-like Polarized Continuum Model (CPCM)[64]. Water ,DMSO and hexane as a solvent were used to compute the free energy of solvation of BQ derivatives at 289K and 1atm.ΔG_{solv} was used to determine solubility and stability of organic molecules. Thermodynamic cycle is reported as a most positive method for redox potential prediction. The thermodynamic cycle displayed in Scheme 1 was used to calculate the Gibbs free energy of the reaction in solution, ΔG^0_{solv}.

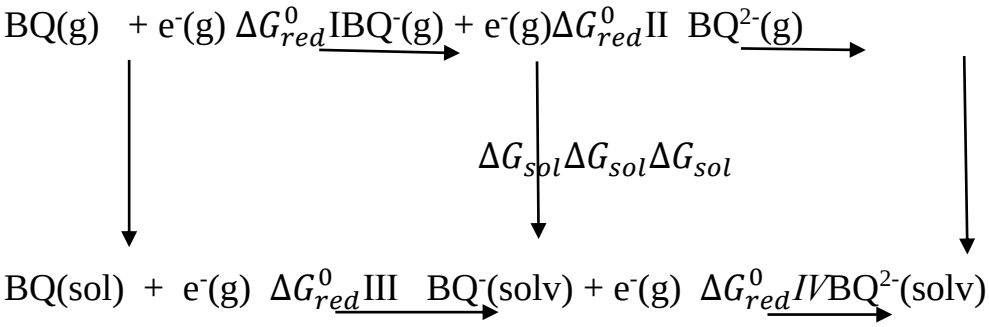

Scheme 1. The thermodynamic quantity used to calculate solvation Gibbs free energy

Where ΔG^0_{red}(sol, BQ^-) andΔG^0_{red} (sol, BQ) is the standard free energy solvation of BQ^- and BQ, respectively, and G^0_{red}(sol, BQ) is the change in the standard free energy of a reaction in the gas phase. The following is the standard free energy of each state in the gaseous phase:

$$\Delta G^0_{red}\ gas = E_{0K} + ZPE + \Delta\Delta G^0_{(298K)} \quad (3.3.3)$$

The energy at 0K is computed by using DFT at optimized geometries while zero-point energy and thermal energy $\Delta\Delta G^0$ at 298K together with entropies were used to convert internal energies to Gibbs free energy at 298K [65]. The above equation is used to convert 1atm to 1M in the ΔG^0 gas state

$$\Delta G\,^0\text{gas(1M)} = \Delta G\,^0\text{gas(1atm)} + RT\ln(24.46) = \Delta G\,^{0\rightarrow *} \quad (3.3.4)$$

The sum of electron affinity and solvation energy is the difference in the Gibbs free energy of a BQ in solution during reduction, according to the aforementioned thermodynamic cycle. The change in BQ's Gibbs free energy during a reduction in the gas phase is referred to as electron affinity, EA (ΔG_{gas}). CPCM solvent model optimized structures of an aqueous phase were used to compute the solvation Gibbs free energy for the particular solution. So, in the solvent phase, the solvation free energy ($\Delta\Delta G_{solv}$) is the change in free energy of BQ due to a state change from neutral to anionic BQ^{-}.

$$\Delta\Delta G_{sol} = \Delta G_{solv}(BQ^-) - \Delta G_{solv}(BQ)_{neu} \quad (3.3.5)$$

Where$\Delta\Delta G^0_{solv}$ the solvation free energy, is$\Delta G^0_{solv}(BQ)^-$ solvation energy of anionic species in a solution, and$\Delta G^0_{SOlv}(BQ)$ is denoted the solvation-free energy of a neutral species. A negative value ofΔG^0_{solv} indicates a Quinone with good aqueous solubility.

To determine the standard free energy (ΔG^0 gas), the molecular structures of BQ andBQ^- were independently optimized at the hybrid functional, B3LYP/6-311G/d level of theory. As a result, the difference between BQ-(anion) and BQ (neutral) in the gas phase is the change in free energy in the gas phase. The solvation free energy of BQ and BQ- using the C-PCM solvent model was also determined in the same way as the gas-phase free energy calculation. The standard Gibbs free energy of BQ (aq) and $BQ^-(aq)$was then calculated using vibrational frequency calculations. In this phase of the calculations, the standard free energy of an electron, is equal to zero at all temperature [66].

The redox potential, ΔE^{red} of active positive electrode material in solution with respect to a Li/Li+ reference electrode can be predicted by the following Equation as [67]

$$\Delta E^{red} = -\frac{\Delta G_{sol}}{nF} - 1.24\text{V} \quad (3.3.6)$$

Where, ΔG_{Sol} is the difference in Gibbs free energy in solution upon reduction (eV), n is the number of electrons transferred and F is the Faraday constant (96500 C/mole). The constant 1.24V indicate the redox potential of the Li/Li+ reference electrode [(-4.28 V [68, 69] SHE (-

3.04 V) Li/Li+]. All redox potential in this paper is reported with the reference to Li/Li+ unless mentioned otherwise. The electronic properties i.e., HOMO and LUMO energy levels, as well as the electron affinity of the active positive electrode materials, were also computed to rationalize the predicted redox potentials Correlation of electro-affinity-solvation energy-redox potentials: according to the thermodynamic cycle, the difference in Gibbs free energy of Quinone in the solution phase during reduction is defined as the sum of electro-affinity and solvation energy [70, 71]. For all Gaussian types, energy would be given in atomic units. The SI unit of the atomic unit is Hartree and with energy relationship as follows:

1Hartree= 627.15 Kcal/mole =2625.50 KJ/mole = 27.212 eV

Finally, properties including HOMO/LUMO energies, vertical ionization potential (IP), electro-affinity (EA), and band-gap (E_g) are derived through energy calculation performed at the B3LYP/6-311/G/d level of theory.

CHAPTER FOUR

4. RESULTS AND DISCUSSION

4.1. Geometry optimization

The geometry optimization of a molecule is the most important step for the computation of redox potential, the ground state of molecular parameterized were controlled by molecular geometry. The molecular structure of BQ derivatives is summarized in scheme 2 below.
The minimum energy was calculated using molecular information from the gas view as an input file. The studied compound's molecular energies were calculated using Gaussian 09 at DFT, with the B3LYP hybrid functional and the 6-311G/d basis set, and a single point energy calculation. To confirm the existence of an energy minimum, the vibrational frequency was examined.

	Optimized structure of BQ and its derivatives	
	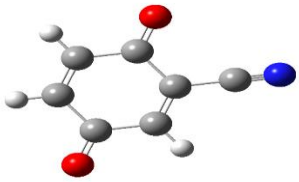 2-Cyano-1,4-BQ	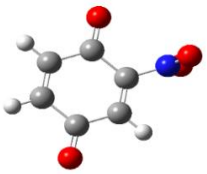 2-Nitro-1,4-BQ
	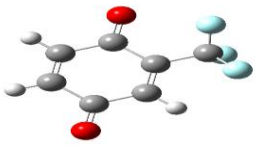 2-Methyltriflouro -1,4-Benzoquinone	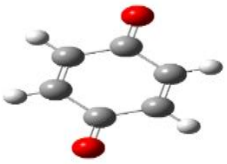 1,4-Benzoquinone

		
	2-methylketone-1,4-BQ	2-acyl-1,4-BQ

Figure 5. optimized structures of BQ and its derivative

4.2. Solvent effect

The most essential element in determining the theoretical redox potentials of BQ is the Solvation effect. The DFT employing hybrid functional B3LYP and 6-311G/d basis set was used to investigate the target molecule's solvent effect. The solvation-free energy equivalent to 1atm and 298K at the standard state is calculated using the CPCM model. Different electron-withdrawing groups of benzoquinone derivatives are represented in Scheme 2.

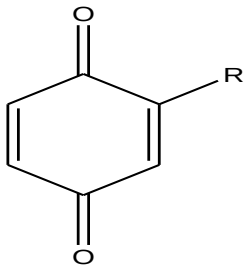

R= -H
= -NO_2
= -$COOCH_3$
= -CF_3
= -CN
= -$COCH_3$
= -CHO

Scheme 2 Structural features of BQ derivatives.

The effect of the solvent on the first and second reduction potentials of substituted BQs were inveterate by comparing the computed solvation-free energy of BQ as shown in figure (6). The first and second reduction potentials in three different solvents with differing dielectric constants are shown in diagram below. Both the first reduction potential, as well as the second reduction potential, is increasing with dielectric constants. Different interactions

between different kinds of neutral, monoanionic, and dianion BQ derivatives with a solvent can be linked to this reduction potential.

The solvation free energy change of molecules as their phase transitions from gaseous neutral species to anionic state in a solvent is known as the solvent effect. A simple equation can be used to express the solvation free energy.

$$\Delta\Delta G_{sol} = \Delta G_{sol}(BQ^{-}) - \Delta G_{sol}\,(BQ)_{neu.}$$

Where, $\Delta\Delta G_{sol}$denotes solivation free energies of solutions.

$\Delta G_{sol}(BQ^{-})$ denotes solivation free energies of BQ anion.

$\Delta G_{sol}(BQ)$ denotes solivationfree energies ofneutral BQ.

A lower solvation free energy value suggests that the transition from neutral to anionic state is more favourable.

Table 1. The free energies of solvation(ΔG_{solv}) of BQ derivatives using water, dimethylsulphoxide and n-hexane

	BQ & its derivatives	ΔG_{sol}(Kcal/mole)		
		Water	DMSO	n-hexane
1	2-NO_2-1,4-BQ	-103.03	-105.74	-82.43
2	2-CN-1,4-BQ	-102.00	-101.66	-80.67
3	2-CF_3-1,4-BQ	-98.40	-98.02	-76.16
4	2-$COOCH_3$-1,4-BQ	-96.44	-96.02	-71.73
5	2-$COCH_3$-1,4-BQ	-95.30	-94.67	-76.73
6	1,4-BQ	-91.11	-90,70	-65.15
7	2-CHO-1,4-BQ	-99.00	-99.57	-73.73
	Average	-97.90	-98.05	-75.23

1	2-OH-1,4-BQ	-91.25	-90.86	-58.84
2	2-NH_2-1,4-BQ	-89.36	-88.94	-58.96
	Average	-90.31	-89.9	-58.90

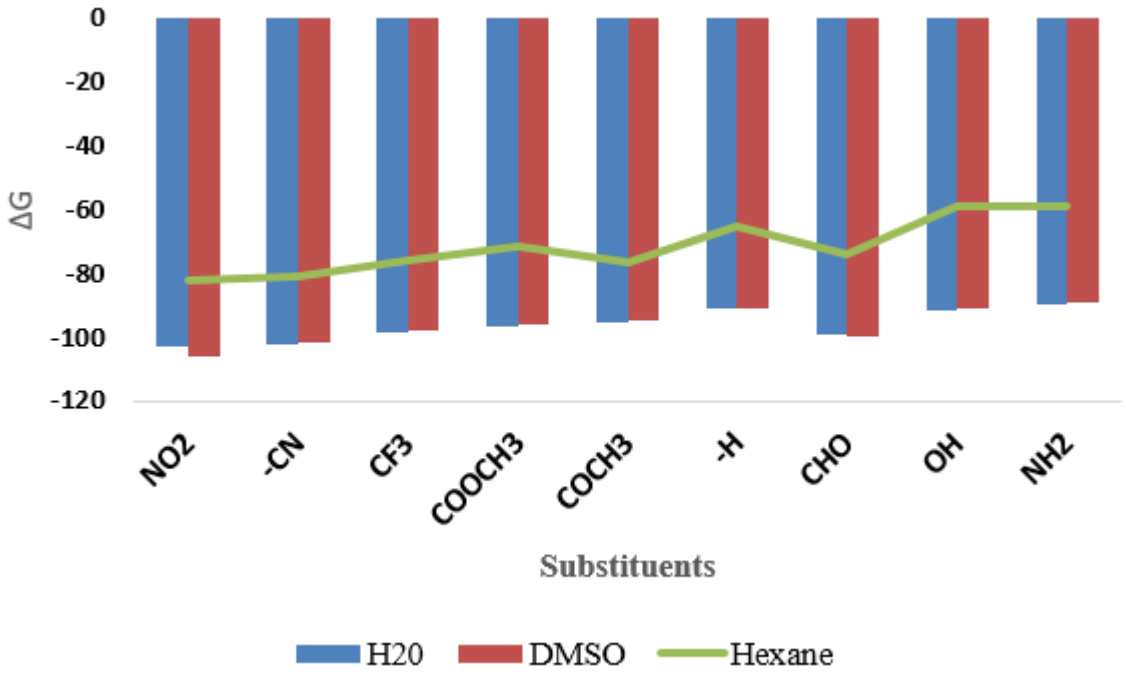

Figure 6. The free energies of solvation(ΔG_{solv}) of BQ derivatives using water, dimethylsulphoxide and n-hexane

Benzoquinones were investigated electrochemically in three solvents: DMSO, hexane and water molecules. In the gas phase, Gibb's free energies for the neutral, monoanionic, and dianions produced by BQ derivatives were calculated. The related solvation free energies, consisting of electrostatic and non-electrostatic components, were computed using the CPCM solvent model to obtain the Gibbs free energies of the studied molecule for the redox process. In the table above, the computed average solvation free energies for the three solvents are labeled. Trends in free energy of solvation for the three solvents of BQ derivatives were: n-hexane<<DMSO $\approx H_2O$. This is due to the investigated compound's polarity, hydrogen bonding (especially for water), and increased dielectric constant.

The solvation free energies ($\Delta(\Delta G^0_{solv})$) with respect to the parent quinone after quinone functionalized with EWGs (-CHO,-$COCH_3$,-$COOCH_3$,-CF_3, -CN, -NO_2),the negative value of $\Delta(\Delta G^0_{solv})$ shows an increase in solubility.

The solvation-free energy of water and DMSO molecules is larger than the non-polar hexane solvents, as can be seen in the table above. One of the most important factors in determining a solute's solubility is its solvation-free energy [72]. Higher solvation free energy suggests a more favorable interaction of the electron-withdrawing group with the aqueous solvent (water) and DMSO molecules, implying greater solubility. The solvation free energy of electron-withdrawing groups, such as the nitro and cyano-group, is higher than other electron-withdrawing groups and bare BQ in all three solvent media. As a result, adding those groups to the functionalization of BQ can improve the interaction between the solute and the organic/inorganic solvent. Because the solvent phase influences the redox potential through the solvation effect and electro-affinity [73], the effect of the solvent phase's dielectric constant on the redox potential was also addressed.

The change in redox potential was calculated for a wide range of dielectric constants1.88, 46.83 and 78.36, for hexane, dimethyl-sulphoxide and water respectively. The average solvation free energy of water (-97.90 Kcal/mole) and DMSO (-98.05 Kcal/mol) with comparable solvation free energy and higher than hexane (-75.23Kcal/mol).

EDGs, such as -OH and NH_2 substituted BQ show a decrease in solvation free energy than BQ substituted with EWGs. This is due to the difference in their electronic activity and dielectric constants of the solvents.

The dielectric constant has a comparable influence on the redox potential for BQ functional group. The redox potential rises from a low dielectric constant to a high dielectric constant, and it stays constant beyond a certain point.

4.3. Theoretical first and second Reduction Potential Analysis

Correlation of electron affinity – solvation energy – redox property: previous studies on the Li-based redox properties of Quinones and carbon materials have shown two main features [76], [77]. (i) Organic molecules would sustain the cathodic activity exhibiting positive redox potentials until each carbonyl could bind with one Li and thereby no carbonyl is available for further Li binding. (ii) The cathodic activity would strongly rely on the solvation energy. Organic molecules with negative solvation energy (i.e., solvation-free energy at the neutral state >solvation-free energy at the anion state) would be cathodically active exhibiting

positive redox potentials. Thus, the correlations of three key components, namely, solvation energy, EA and redox property, were carefully investigated in three approaches to study fundamental structure-property relationships. Therefore, correlating the redox properties of the seven quinone derivatives with their electronic structures, such as the EA, lowest unoccupied molecular orbital (LUMO), and highest occupied molecular orbital (HOMO).

The redox potential of a molecule is a measurement of its tendency to gain or lose electrons. One of the most common approaches to calculate redox potentials is the use of a thermodynamic cycle that involves the gas phase energies and free energies of solvation [74–78]. The first and second electron reduction potentials of the benzoquinone-containing electron-withdrawing group were calculated using the B3LYP level of theory at the 6-311G/d basis specified in the equation (3.3.6). The CPCM approach, which was successfully applied to calculate BQ reduction potentials, also employed for the explanation of the solvent effect

Table 2. Computed first (E^1_{red}V and second (E^2_{red} V) the reduction potential of various BQ derivatives at the B3LYP/6-311G (d) level of theory.

BQ& its derivatives substituent effect	Theoretical first &second reduction potentials of BQ Derivatives					
	Water (ε = 78.36)		DMSO (ε =46.83)		C_6H_{14}(ε=1.88)	
	E^1_{red}	E^2_{red}	E^1_{red}	E^2_{red}	E^1_{red}	E^2_{red}
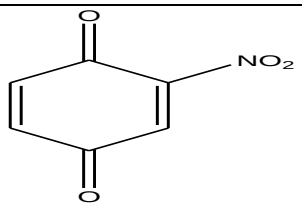	3.27	2.75	3.35	2.34	2.32	0.59
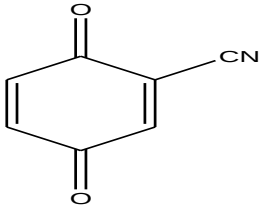	3.19	2.41	3.14	2.38	2.26	0.69
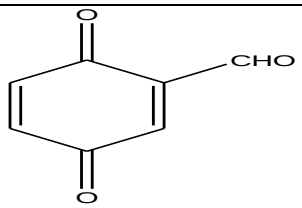	3.03	2.08	3.14	2.35	1.99	0.34

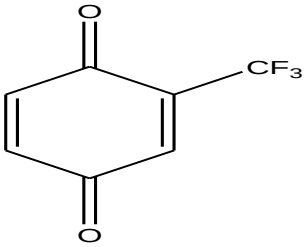	3.02	2.27	3.01	2.22	2.06	0.21
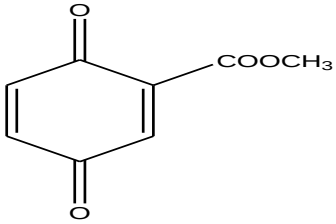	2.94	2.21	2.93	2.17	1.83	0.16
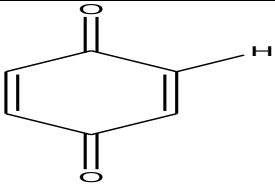	2.71	1.99	2.69	1.88	1.44	0.16
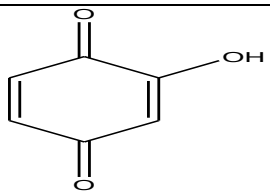	2.71	1.99	2.70	1.91	1.29	0.16
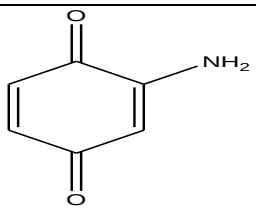	2.64	2.05	2.62	2.01	1.32	0.68
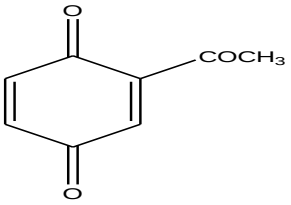	**2.90**	**2.32**	**2.87**	**2.30**	**1.87**	**0.15**

Using quantum mechanics, the electrochemical behaviour of BQ and its derivatives was examined in three different solvents via C_6H_{14}, DMSO and water. The first step reduction potential from n-hexane to water increases. This is due to hydrogen bonding, HOMO-LUMO energies, the dielectric constant and polarity of the solvent as shown below.

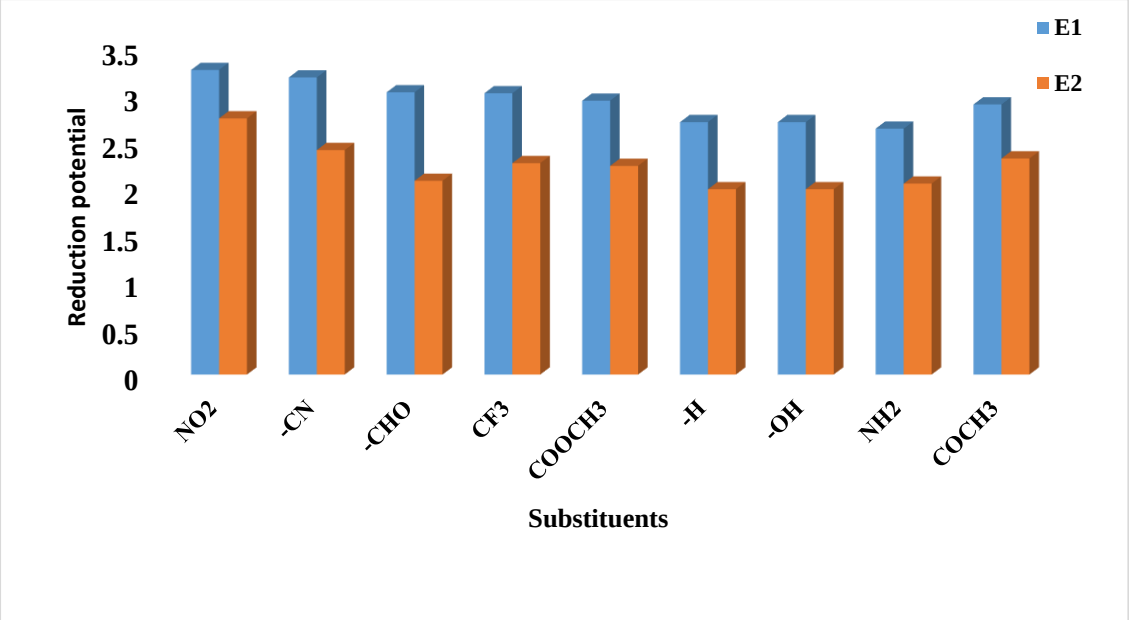

Figure 7. The first and second reduction potential of BQ and its substituent in water at B3LYP/DFT Using at 6-311/G (d) level of theory

The above figure shows the theoretical reduction potential of benzoquinone derivatives. The first and second theoretical reduction potential of benzoquinone molecule increase, when EWGs such as -CHO, $-COCH_3$, $-COOCH_3$, $-CF_3$, –CN, $-NO_2$ are substituted for quinone hydrogen adjacent to the ketone unit. This is because the two oxygen atoms at the ortho position maximize the reduction potential both in gas and solvent cases.

4.4. Effects of a functional group on the reduction potential of BQ

The electronic properties of extra-functional groups influence the redox properties of the studied molecule [22],[79]. The electronic effects of functional groups on BQ's redox window are critical for expecting active compounds' redox features the characteristics. The

redox behaviours of the new redox-active molecule were assessed using the quantum chemical electronic structure of atoms/molecules. The redox potential is calculated using the CPCM model and the DFT/B3LYP methods for structures with various substituents. The redox potentials on the researched molecule were evaluated in water, DMSO and hexane to compare the redox potentials of bare benzoquinone and the substituted BQs. The nitro and cyano-substituents have higher redox potentials in all three solvents among the electron-withdrawing groups mentioned in scheme 1.

As indicated in Table 2, the computed first (E_{red}^{1}) and second (E_{red}^{2}) reduction potentials of benzoquinone and functional group substituted benzoquinone with no salt molecules were examined. All of these functional groups are electron-withdrawing, and their overall influence on benzoquinone's redox characteristics is predetermined. For example, the first and second reduction potentials of bare benzoquinone are 2.71 V vs. Li/Li+ (standard reduction potential without Li/Li+,3.95 V) and 1.99 V vs Li/Li+ (standard reduction potential without Li/Li+,3.23 V), respectively. This value is a good agreement with the previously theoretically calculated reduction potential of benzoquinone 2.65V and 2.01V, respectively.

4.5. HOMO-LUMO energies

Using the B3LYP hybrid functional with the 6-311G (d) basis set, the energies of the highest occupied molecular orbital (HOMO) and lowest unoccupied molecular orbital (LUMO) of the benzoquinone molecule and its electron-withdrawing group in the ground states are calculated. Chemical stability is determined by both HOMO and LUMO energies. A molecule's chemical reactivity is represented by the energy differential between them. According to Sajan and colleagues, frontier molecular orbital analysis was used to explain the optical and electrical properties of organic molecules [80]. The chemical reactivity of a molecule is influenced by the HOMO-LUMO energies. During a chemical reaction, HOMO is the ability to donate an electron during a chemical process, and its energy is proportional to the ionization potential, (IP). The tendency of a species to donate electrons to the acceptor molecule of an unfilled molecular orbital is indicated by a high homo energy value of a molecule.

The charge transfer interaction within a benzoquinone molecule can be determined by the energy gap between LUMO-HOMO [81]. The most likely place for an electron to be excited is in the energy gap between them. The decreased HOMO-LUMO gap is caused by the delocalization of pi-electrons, making it simple for an electron to go from the lowest energy

level to a higher energy level with a similar energy level. In a large conjugate pi orbital system, the higher the mobility of the pi-electron, the more energy is distributed throughout the molecule to stabilize it. The smaller the HOMO-LUMO gap, the more stability of the studied compounds. The chemical X= -CF_3, -NO_2, and -CN; are relatively more stable (less reactive) than X= -CHO; as indicated in the table below. The -CHO substituent has the lowest energy gap in both the solvent and gas phases, and so increases the reactivity of benzoquinone molecules. Thus, the HOMO-LUMO gap of the electron-withdrawing group on benzoquinone at three different solvent and gas phases is/was illustrated as follows.

Table 3**.** The HOMO-LUMO energy gap is computed at B3LYP/6-311G (d) level.

BQ & its Substituents	Parameters				
	HOMO(eV)	LUMO(eV)	ΔE(eV)	IP(eV)	EA(eV)
GAS (ε=0)					
1. BQCN	-8.13	-4.28	3.85	8.13	4.28
2. $BQNO_2$	-8.09	-4.32	3.77	8.09	4.32
3. $BQCF_3$	-8.02	-4.18	3.84	8.02	4.18
4. BQ	-7.60	-3.93	3.87	7.60	3.93
5. $BQCOOCH_3$	-7.51	-3.88	3.63	7.51	3.88
6.$BQCOCH_3$	-7.45	-4.08	3.37	7.45	4.08
7. BQCHO	-7.31	-4.16	3.15	7.31	4.16
C_6H_{14}(ε =1.88)					
1. BQCN	-8.10	-4.29	3.81	8.10	4.29
2. $BQNO_2$	-8.09	-4.32	3.77	8.09	4.32
3. $BQCF_3$	-7.96	-4.10	3,86	7.96	4.10
4. BQ	-7.59	-3.70	3.89	7.59	3.70
5. $BQCOOCH_3$	-7.38	-3.89	3.47	7.38	3.89
6.$BQCOCH_3$	-7.45	-4.08	3.37	7.45	4.08

7. BQCHO	-7.02	-3.87	3.15	7.02	3.87
DMSO(ε=46.83)					
1 BQCN	-8.02	-4.14	3.88	8.02	4.14
2 $BQNO_2$	-7.83	-4.26	3.57	7.83	4.26
3 $BQCF_3$	-7.89	-3.98	3.91	7.89	3.98
4 BQ	-7.59	-3.66	3.93	7.59	3.66
5 $BQCOOCH_3$	-7.54	-3.87	3.67	7.54	3.87
6. $BQCOCH_3$	-7.22	-3.81	3.41	7.22	3.81
7 BQCHO	-7.23	-3.99	3.24	7.23	3.99
Water (ε=78.36)					
1 BQCN	-8.01	-4.13	3.88	8.01	4.13
2 $BQNO_2$	-7.82	-4.26	3.56	7.82	4.26
3 $BQCF_3$	-7.89	-3.98	3.91	7.89	3.98
4 BQ	-7.59	-3.66	3.93	7.59	3.66
5 $BQCOOCH_3$	-7.40	-3.90	3.50	7.40	3.90
6 $BQCOCH_3$	-7.20	-3.81	3.41	7.22	3.81
7 BQCHO	-7.23	-3.81	3.42	7.23	3.81

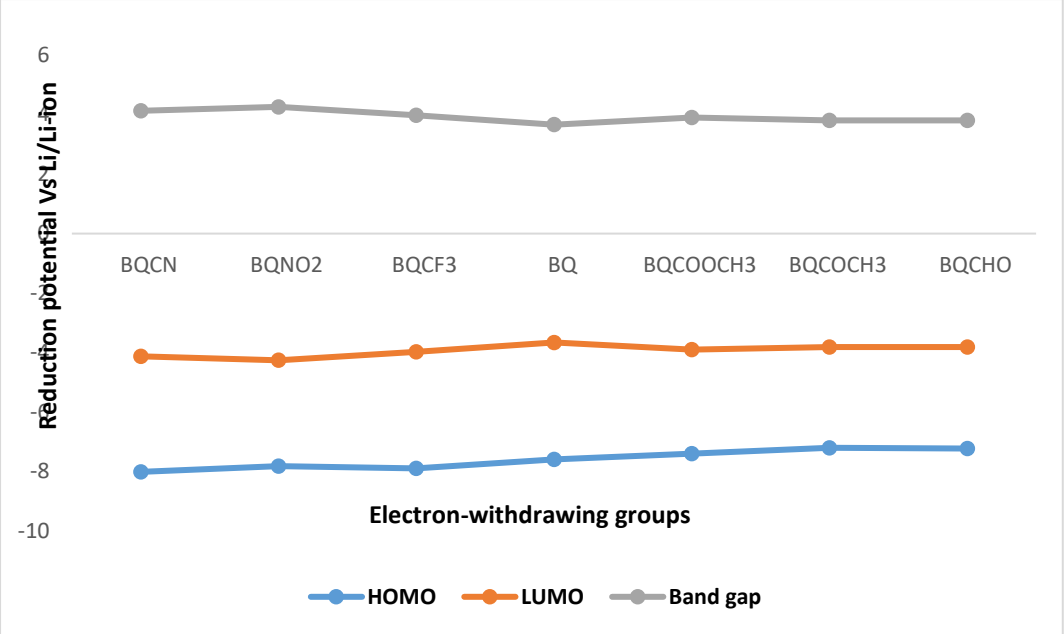

Figure 8. Shapes of the HOMO and LUMO orbitals of compounds 1-7 at the DFT/B3LYP/6-311/G/d level

The chemical activity of the BQ molecule is reflected in the HOMO-LUMO gap above. The charge transfer interaction inside the investigated molecule is shown by a decrease in the HOMO-LUMO gap. The stability of the investigated chemical is arranged as 4>1>3>2>5>6 in gas, 4 > 3 > 1 > 2 > 5 > 6 solvent in (water) and 4 > 3 > 1 > 5 > 2 > 6 in DMSO respectively. Chemical reactivity, on the other hand, decreases in the reverse order,4 < 3 < 1 < 2 < 5 < 6. Compounds 4 and 6 have the highest and lowest solvent and gas-phase stabilities, respectively, according to the theoretical computed result. The chemical reactivity of the investigated molecule, on the other hand, was affected oppositely.

At the B3LYP/6-311G/d level of theory, the FMOs of the studied compound from 1-7 have been computed. The corresponding energy levels of the frontier molecular orbital for the compounds are shown in the figure below. Based on the frontier molecular orbital investigation, electron transfer would occur between HOMO and LUMO.

NO	HOMO energy in eV	LUMO energy in eV
1	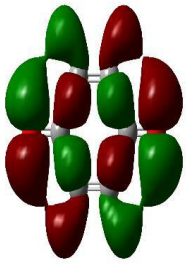 BQ, E= -7.59eV	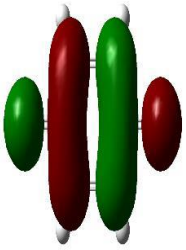 BQ, E= -3.66eV
2	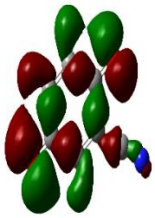 BQCN HOMO; E= -8.01eV	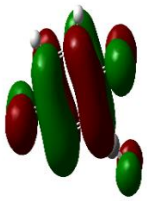 BQCN LUMO; E= -4.13eV
3	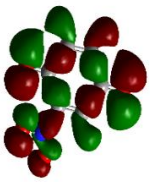 $BQNO_2$ HOMO: E= -7.82eV	 $BQNO_2$ LUMO E= -4.26eV
4	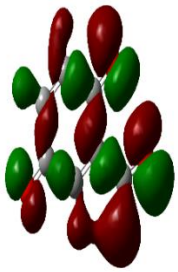 BQCHO, HOMO E= -7.32eV	 BQCHO, LUMO E= -3.81eV

5	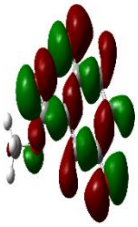 BQCOOCH$_3$, HOMO E= -7.40 eV	 BQCOOCH$_3$, LUMO E= -3.90 eV
6	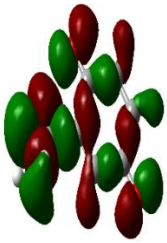 BQCOCH$_3$HOMO E= -7.22 eV	 BQCOCH$_3$ LUMO E= -3.81eV
7	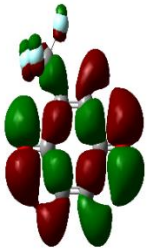 BQCF$_3$HOMO E= - 7.89eV	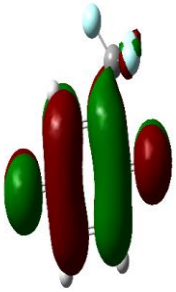 BQCF$_3$ LUMO E= -3.98eV

Figure 9. the computed HOMO-LUMO energies of BQ derivatives at the B3LYP/DFT level of theory using a 6-311G/d basis set.

From scheme 4, it seems that the linear correlations of the redox potential with the LUMO, HOMO, and HOMO-LUMO gap were observed within the range of positive redox potentials. It was particularly highlighted that the more negative values for LUMO, a HOMO would have higher redox potentials for quinines' with more reductive ability while the more positive value of the HOMO-LUMO gap would be related to higher redox potential. Similar observations had been consistently reported from other studies and in table 4 mentioned above [67],[68].

CHAPTER FIVE

5. CONCLUSION AND RECOMMENDATIONS

5.1. Conclusion

In conclusion, the results of this investigation reveal that the electrochemical behaviours of BQ derivatives are substantially influenced by the solvent effect, which is in turn influenced by the solvation-free energy.

1. Solvation model: there are several solvation model widely used to study the solvation effect in computational methods. For this study the CPCM solvation model is recommended for redox potential calculations and the result obtained is consistent with previous experimental result for BQ

2. The molecule BQ-CHO (6) has a low HOMO-LUMO energy gap in chosen gas and solvent phases, making it kinetically less stable. Compounds (6) have a high chemical reactivity in various solvents and the gas phase. And hence the smallest HOMO-LUMO gap, indicating that it has interesting electronic properties.

3. It is noted that using the implicit solvent method that the solvent phase has an effect on the redox properties of BQ derivatives: a solvent phase (in case water) with a high dielectric constant can increase the reduction potential of BQ derivative.

4. Along our expectation of electron withdrawing and donating effects, there is a redox Potential increase for BQ derivatives with-NO_2, - CN, -CF_3, -CHO, -$COOCH_3$, and -$COCH_3$ substituents compared to BQ, whereas decrease for BQ derivatives with -OH, -NH_2, substituents. This is because of increase or decrease of the electron density of the redox center. EDGs increases electron density in the redox center and hence, the redox potential shifts to the negative direction. Whereas EWGs lowers the electron density of the redox center shifting the redox potential to the positive direction.

5.2. RECOMANDATION

Based on the theoretical investigation of the reduction potential of benzoquinone and its derivatives, we recommended the following for studying in the future.

1. The calculated redox potential of the studied molecule was done at B3LYP/DFT theory at a 6-311G/d basis set the conductor-like polarizable continuum model (C-PCM) approach was used to include the role of the solvents. Based on this parameter the introduction of an electron-withdrawing group for example -NO_2, -CN and -CF_3 functional group, has higher redox potential than other electron-withdrawing groups. However, we recommend applying different higher parameters of basis set and other solvation models.
2. Stability is crucial for the performance and permanency of aqueous organic redox flow battery. For further studies, if electrolyte additives were used to enhance the stability and results in increasing the reduction potential.
3. The redox potential of the studied compound can be calculated only based on theoretical methods. For further studies, if it were done additionally in collaboration with experimental, it is better to get more accurate reduction potentials.

APPENDIX -1

Supplementary materials

Figure A1 Renewable energy sources

Figure A2 Redox flow battery applications

REFERENCES

[1].Energy Information Administration US, International Energy Outlook 2019, available from:http://www.informaworld.com/openurl?genre¼article&doi¼10.1080/01636609609550217&magic¼crossref.

[2]. Zhang, H.; Sun, C. Cost-effective iron-based aqueous redox flow batteries for large-scale energy storage application: A review. J. Power Sources **2021**,493, 229445. [CrossRef]

[3]. Sun, C.; Negro, E.; Vezzù, K.; Pagot, G.; Cavinato, G.; Nale, A.; Herve Bang, Y.; Di Noto,V. Hybrid inorganic-organic proton conducting Membranes based on SPEEK doped with WO_3Nano-particles for application in vanadium redox flow batteries. Electrochim. Acta, 2019, 309, 311–325. [CrossRef]

[4]. Yan, R., & Wang, Q. (2018). Redox-targeting-based flow batteries for large-scale energy storage. *Advanced Materials*, *30*(47), 1802406.

[5]. Winsberg, J., Hagemann, T., Janoschka, T., Hager, M. D., & Schubert, U. S. (2017). Redox-flow batteries: from metals to organic redox-active materials. *Angewandte Chemie International Edition*, *56*(3), 686-711.

[6]. Y. Ding, C. Zhang, L. Zhang, Y. Zhou, and G. Yu, Chem. Soc. Rev., 47, 69 (2018).
Ding, Y., Zhang, C., Zhang, L., Zhou, Y., & Yu, G. (2018). Molecular engineering of organic electroactive materials for redox flow batteries. *Chemical Society Reviews*, *47*(1), 69-103.

[7]. Luo, J., Hu, B., Hu, M., Zhao, Y., & Liu, T. L. (2019). Status and prospects of organic redox flow batteries toward sustainable energy storage. *ACS Energy Letters*, *4*(9), 2220-2240.

[8]. Li, W., Fu, H. C., Li, L., Cabán-Acevedo, M., He, J. H., & Jin, S. (2016). Integrated photoelectrochemical solar energy conversion and organic redox flow battery devices. *Angewandte Chemie*, *128*(42), 13298-13302.

[9]. Zhang, C., Niu, Z., Bae, J., Zhang, L., Zhao, Y., & Yu, G. (2021). Polyeutectic-based stable and effective electrolytes for high-performance energy storage systems. *Energy & Environmental Science*, *14*(2), 931-939.

[10]. Ding, Y., & Yu, G. (2017). The Promise of Environmentally Benign Redox Flow Batteries by Molecular Engineering. *Angewandte Chemie (International ed. in English)*, *56*(30), 8614-8616.

[11]. Kwabi, D. G., Ji, Y., & Aziz, M. J. (2020). Electrolyte lifetime in aqueous organic redox flow batteries: a critical review. *Chemical Reviews*, *120*(14), 6467-6489.

[12]. Zhang, C., Ding, Y., Zhang, L., Wang, X., Zhao, Y., Zhang, X., & Yu, G. (2017). A Sustainable Redox-Flow Battery with an Aluminum-Based, Deep-Eutectic-Solvent Anolyte. *Angewandte Chemie International Edition*, *56*(26), 7454-7459.

[13]. Yang, Z., Zhang, J., Kintner-Meyer, M. C., Lu, X., Choi, D., Lemmon, J. P., & Liu, J. (2011). Electrochemical energy storage for green grid. *Chemical reviews*, *111*(5), 3577-3613.

[14]. Soloveichik, G. L. (2015). Flow batteries: current status and trends. *Chemical reviews*, *115*(20), 11533-11558.

[15]. Wang, W., Luo, Q., Li, B., Wei, X., Li, L., & Yang, Z. (2013). Recent progress in redox flow battery research and development. *Advanced Functional Materials*, *23*(8), 970-986.

[16]. Zhong, F., Yang, M., Ding, M., & Jia, C. (2020). Organic electroactive molecule-based electrolytes for redox flow batteries: status and challenges of molecular design. *Frontiers in Chemistry*, *8*, 451. DOI: 10.3389/fchem.2020.00451.

[17]. Pan, F., & Wang, Q. (2015). Redox species of redox flow batteries: A review. *Molecules*, *20*(11), 20499-20517.

[18]. Singh, V., Kim, S., Kang, J., & Byon, H. R. (2019). Aqueous organic redox flow batteries. *Nano Research*, *12*, 1988-2001.

[19]. Luo, J., Hu, B., Hu, M., Zhao, Y., & Liu, T. L. (2019). Status and prospects of organic redox flow batteries toward sustainable energy storage. *ACS Energy Letters*, *4*(9), 2220-2240.

[20]. Hu, B., DeBruler, C., Rhodes, Z., and Liu, T. L. (2017). Long-cycling aqueous organic redox flow battery (AORFB) toward sustainable and safe energy Storage. J. Am. Chem. Soc. 139, 1207–1214. doi:10.1021/jacs.6b10984

[21]. Beh, E. S., De Porcellinis, D., Gracia, R. L., Xia, K. T., Gordon, R. G., & Aziz, M. J. (2017). A neutral pH aqueous organic–organometallic redox flow battery with extremely High-capacity retention. *ACS Energy Letters*, *2*(3), 639-644.

[22]. DeBruler, C., Hu, B., Moss, J., Liu, X., Luo, J., Sun, Y., & Liu, T. L. (2017). Designer two-electron storage viologen anolyte materials for neutral aqueous organic redox flow batteries. *Chem*, *3*(6), 961-978.

[23]. Er, S., Suh, C., Marshak, M. P., & Aspuru-Guzik, A. (2015). Computational design of molecules for an all-quinone redox flow battery. *Chemical science*, *6*(2), 885-893.

[24]. Wedege, K., Dražević, E., Konya, D., & Bentien, A. (2016). Organic redox species in aqueous flow batteries: redox potentials, chemical stability and solubility. *Scientific reports*, *6*(1), 39101.

[25]. Hofmann, J. D., Pfanschilling, F. L., Krawczyk, N., Geigle, P., Hong, L., Schmalisch, S., ... & Schröder, D. (2018). Quest for organic active materials for redox flow batteries: 2, 3-diaza-anthraquinones and their electrochemical properties. *Chemistry of Materials*, *30*(3), 762-774.

[26]. Hofmann, J. D., Schmalisch, S., Schwan, S., Hong, L., Wegner, H. A., Mollenhauer, D., ... & Schröder, D. (2020). Tailoring dihydroxyphthalazines to enable their stable and efficient use in the catholyte of aqueous redox flow batteries. *Chemistry of Materials*, *32*(8), 3427-3438.

[27] Y,Song and G.R. Buettner, Free Radical Biol.-Med.,2010 ,49,919 962 CrossRef .

[28]. Hammett, L. P. (1937). Chem. Reviews 17, 125 (1935); LP Hammett. *J. Amer. chemrSbc*, *59*, 96.

[29]. Zhu, X. Q., & Wang, C. H. (2010). Accurate estimation of the one-electron reduction potentials of various substituted quinones in DMSO and CH3CN. *The Journal of organic chemistry*, *75*(15), 5037-5047.

[30]. Han, C., Li, H., Shi, R., Zhang, T., Tong, J., Li, J., & Li, B. (2019). Organic quinones towards advanced electrochemical energy storage: recent advances and challenges. *Journal of Materials Chemistry A*, *7*(41), 23378-23415.

[31] D.Ajloo, B. Yoonesi and A. Soleymanpour, int.,J. Electrochem,sci,2010,5,459-477.CAS

[32]. Chen, C., Zhang, S., Zhu, Y., Qian, Y., Niu, Z., Ye, J,…. & Zhang, X. (2018). Pyridyl group design in viologens for anolyte materials in organic redox flow batteries. RSC advances, 8(34), 18762-18770.

[33]. Luo, J., Hu, B., Hu, M., Zhao, Y., & Liu, T. L. (2019). Status and prospects of organic redox flow batteries toward sustainable energy storage. *ACS Energy Letters*, *4*(9), 2220-2240.

[34]. Darling, R. M., Gallagher, K. G., Kowalski, J. A., Ha, S., & Brushett, F. R. (2014). Pathways to low-cost electrochemical energy storage: a comparison of aqueous and nonaqueous flow batteries. *Energy & Environmental Science*, *7*(11), 3459-3477.

[35]. Leung, P., Shah, A. A., Sanz, L., Flox, C., Morante, J. R., Xu, Q., ... & Walsh, F. C. (2017). Recent developments in organic redox flow batteries: A critical review. *Journal of Power Sources*, *360*, 243-283, https://doi.org/10.1016/j.jpowsour.2017.05.057.

[36]. Dmello, R., Milshtein, J. D., Brushett, F. R., & Smith, K. C. (2016). Cost-driven materials
selection criteria for redox flow battery electrolytes. *Journal of Power Sources*, *330*, 261-272.

[37]. Wei, X., Pan, W., Duan, W., Hollas, A., Yang, Z., Li, B…..& Sprenkle, V. (2017).

Materials and systems for organic redox flow batteries: status and challenges. *ACS Energy Letters*, *2*(9), 2187-2204. https://doi.org/10.1021/acsenergylett.7b00650.

[38]. Suo, L., Borodin, O., Wang, Y., Rong, X., Sun, W., Fan, X., ... & Wang, C. (2017). "Water-in-salt" electrolyte makes aqueous sodium-ion battery safe, green, and long-lasting. *Advanced Energy Materials*, *7*(21), 1701189.

[39]. Badwal, S. P., Giddey, S. S., Munnings, C., Bhatt, A. I., & Hollenkamp, A. F. (2014). Emerging electrochemical energy conversion and storage technologies. *Frontiers in chemistry*, *2*, 79.

[40]. Alotto, P., Guarnieri, M., & Moro, F. (2014). Redox flow batteries for the storage of renewable energy: A review. *Renewable and sustainable energy reviews*, *29*, 325-335.

[41]. Weber, A. Z., Mench, M. M., Meyers, J. P., Ross, P. N., Gostick, J. T., & Liu, Q. (2011). Redox flow batteries: a review. *Journal of applied electrochemistry*, *41*, 1137-1164.

[42]. Soloveichik, G. L. (2015). Flow batteries: current status and trends. *Chemical reviews*, *115*(20), 11533-11558.

[43]. Yu, J., Zhao, T. S., & Pan, D. (2020). Tuning the performance of aqueous organic redox flow batteries via first-principles calculations. *The Journal of Physical Chemistry Letters*, *11*(24), 10433-10438.

[44]. Gupta, N., & Linschitz, H. (1997). Hydrogen-bonding and protonation effects in electrochemistry of quinones in aprotic solvents. *Journal of the American Chemical Society*, *119*(27), 6384-6391.

[45]. Isegawa, M., Neese, F., & Pantazis, D. A. (2016). Ionization energies and aqueous redox potentials of organic molecules: comparison of DFT, correlated ab initio theory and pair natural orbital approaches. *Journal of Chemical Theory and Computation*, *12*(5), 2272-2284.

[46]. Namazian, M., Zare, H. R., & Yousofian-Varzaneh, H. (2016). Electrochemical behavior of tetrafluoro-p-benzoquinone at the presence of carbon dioxide: Experimental and theoretical studies. *Electrochimica Acta*, *196*, 692-698.

[47]. Baik, M. H., & Friesner, R. A. (2002). Computing redox potentials in solution: Density functional theory as a tool for rational design of redox agents. *The Journal of Physical Chemistry A*, *106*(32), 7407-7412.

[48]. Wang, Y. (2012). Theoretical Studies on Artificial Water Splitting-Water Oxidation and Proton Transfer (Doctoral dissertation, KTH Royal Institute of Technology).

[49] Schrödinger, E. (1926). An undulatory theory of the mechanics of atoms and molecules. *Physical review*, *28*(6), 1049.

[50] Born, M. (1927). Born-oppenheimer approximation. *Ann. Phys*, *84*, 457-484.

[51]. W. Kohn, "Nobel Lecture: Electronic structure of matter-wave functions and density functional *," vol. 71, no. 5, pp. 1253–1266, 1999.

[52]. Contreras, R. R., Almarza, J., & Rincón, L. (2021). Molten carbonate fuel cells: a technological perspective and review. *Energy Sources, Part A: Recovery, Utilization, and Environmental Effects*, 1-15.

[53]. Hohenberg, P., & Kohn, W. J. P. R. (1964). Density functional theory (DFT),Phys. Rev, 136, B864.

[54]. Miyasita, M., Higuchi, K., & Higuchi, M. (2011). Self-Consistent Calculations on the Atomic Electron Affinity and Ionization Energy with Taking Effects of the Nonspherical Distribution of Electrons into Account. *Journal of Modern Physics*, *2*(10), 1161-1165, DOI: 10.4236/jmp.2011.210144.

[55]. Kohn, W. (1986). Density-functional theory for excited states in a quasi-local-density approximation. *Physical Review A*, *34*(2), 737.

[56]. Perdew, J. P., Burke, K., & Ernzerhof, M. (1996).Generalized Gradient Approximation Made Simple. Physical Review Letters,77(18),3865–3868.

[57]. Becke, A. D. (1988). Density-functional exchange-energy approximation with correct asymptotic behavior. Physical review A,38(6), 3098.

[58]. Lee, C., Yang, W., & Parr, R. G. (1988). Development of the Colle-Salvetti Correlation-energy formula into a functional of the electron density. Physical review B, 37(2), 785.

[59]. Perdew, J. P., Ziesche, P., & Eschrig, H. (1991). Electronic structure of solids' 91.

[60]. Tao, J., Perdew, J. P., Ruzsinszky, A., Scuseria, G. E., Csonka, G. I., &Staroverov, V. N. (2007). Meta-generalized gradient approximation: non-empirical construction and Performance of a density functional. Philosophical Magazine, 87(7), 1071–1084. doi: 10.1080/14786430601021660

[61]. Jensen, K. P., & Cirera, J. (2009). Accurate Computed Enthalpies of Spin Crossover in Iron and Cobalt Complexes. The Journal of Physical Chemistry A, 113(37), 10033–10039. doi: 10.1021/jp900654j

[62]. Pérez-Jiménez, A. J., Pérez-Jordá, J. M., Pastor-Abia, L., & Sancho-Garcıa, J. C. (2002). New correlation energy functionals with explicit dependence on the number of electrons. *The Journal of chemical physics*, *116*(24), 10571-10576.

[63] Priya, M. K., Revathi, B. K., Renuka, V., Sathya, S., & Asirvatham, P. S. (2019). Molecular structure, spectroscopic (FT-IR, FT-Raman, 13C and 1H NMR) analysis, HOMO-LUMO energies, Mulliken, MEP and thermal properties of new chalcone derivative by DFT calculation. *Materials Today: Proceedings*, *8*, 37-46.

[64]. A. Manuscript, "rsc.li/pccp," vol. 19, 2019, doi: 10.1039/b000000x/.

[65]. Liptak, M. D., Gross, K. C., Seybold, P. G., Feldgus, S., & Shields, G. C. (2002). Absolute p K a determinations for substituted phenols. *Journal of the American Chemical Society*, *124*(22), 6421-6427.

[66] Winget, P., Cramer, C. J., & Truhlar, D. G. (2004). Computation of equilibrium oxidation and reduction potentials for reversible and dissociative electron-transfer reactions in solution. *Theoretical Chemistry Accounts*, *112*, 217-227. DOI: 10.1007/s00214-004-0577-0.

[67]. Bachman, J. E., Curtiss, L. A., & Assary, R. S. (2014). Investigation of the redox chemistry of anthraquinone derivatives using density functional theory. *The Journal of Physical Chemistry A*, *118*(38), 8852-8860.

[68]. Isse, A. A., & Gennaro, A. (2010). Absolute potential of the standard hydrogen electrode and the problem of interconversion of potentials in different solvents. *The Journal of Physical Chemistry B*, *114*(23), 7894-7899.

[69]. Kelly, C. P., Cramer, C. J., & Truhlar, D. G. (2006). Aqueous solvation free energies of ions and ion− water clusters based on an accurate value for the absolute aqueous solvation free energy of the proton. *The Journal of Physical Chemistry B*, *110*(32), 16066-16081.

[70]. Park, J. H., Liu, T., Kim, K. C., Lee, S. W., & Jang, S. S. (2017). Systematic molecular design of ketone derivatives of aromatic molecules for lithium-ion batteries: First-principles DFT modeling. *ChemSusChem*, *10*(7), 1584-1591,DOI: 10.1002/cssc.201601730.

[71]. Kim, K. C., Liu, T., Lee, S. W., & Jang, S. S. (2016). First-principles density functional theory modeling of Li binding: thermodynamics and redox properties of quinone derivatives for lithium-ion batteries. *Journal of the American Chemical Society*, *138*(7), 2374-2382. DOI:10.1021/jacs.5b13279.

[72]. D. S. Palmer *et al.*, "articles Thermodynamic Cycle," no. 5, pp. 545–556,2008.

[73]. Brus, L. E. (1983). A simple model for the ionization potential, electron affinity, and aqueous redox potentials of small semiconductor crystallites. *The Journal of chemical physics*, *79*(11), 5566-5571.

[74]. Baik, M.H.; Friesner, R.A. Computing redox potentials in solution: Density functional theory as a tool for rational design of redox agents. J. Phys. Chem. A **2002**, 106, 7407–7412. [CrossRef]

[75]. Schmidt am Busch, M.; Knapp, E.W. One-electron reduction potential foroxygen- and Sulfur-centred organic radicals in protic and aprotic solvent J. Am. Chem. Soc. **2005**, 127, 15730–15737. [CrossRef] [PubMed]

[76]. Jaque, P.; Marenich, A.V.; Cramer, C.J.; Truhlar, D.G. Computational electrochemistry: The aqueous Ru3+|Ru2+ reduction potential. J. Phys.Chem. C **2007**, 111, 5783–5799.

[77]. Hodgson, J.L.; Namazian, M.; Bottle, S.E.; Coote, M.L. One-electronoxidation and reduction potentials of nitroxide antioxidants: A theoretical study. J. Phys. Chem. A **2007**, 111, 13595–13605. [CrossRef] [PubMed]

[78]. Marenich, A.V.; Majumdar, A.; Lenz, M.; Cramer, C.J.; Truhlar, D.G.Construction of Pourbaix diagrams for ruthenium-based water-oxidation catalysts by density functional theory. Angew. Chem. Int. Ed. **2012**, 51,12810–12814. [CrossRef] [PubMed]

[79]. Er, S., Suh, C., Marshak, M. P., & Aspuru-Guzik, A. (2015). Computational design of molecules for an all-quinone redox flow battery. *Chemical science*, *6*(2), 885-893.

[80]. Padmaja, L., Ravikumar, C., Sajan, D., Hubert Joe, I., Jayakumar, V. S., Pettit, G. R., & Faurskov Nielsen, O. (2009). Density functional study on the structural conformations and intramolecular charge transfer from the vibrational spectra of the anticancer drug combretastatin-A2. *Journal of Raman Spectroscopy: An International Journal for Original Work in all Aspects of Raman Spectroscopy, Including Higher Order Processes, and also Brillouin and Rayleigh Scattering*, *40*(4), 419-428

[81]. Miar, M., Shiroudi, A., Pourshamsian, K., Oliaey, A. R., & Hatamjafari, F. (2021). Theoretical investigations on the HOMO–LUMO gap and global reactivity descriptor studies, natural bond orbital, and nucleus-independent chemical shifts analyses of 3-phenylbenzo [d] thiazole-2 (3 H)-imine and its para-substituted derivatives: Solvent and substituent effects. *Journal of Chemical Research*, *45*(1-2), 147-158,. DOI:10.1177/1747519820932091.